Covalent Functionalization of Short, Single-Wall Carbon Nanotubes: Photophysics of 2,4,6-Triphenylpyrylium Attached to the Nanotube Walls

ARTICLE *in* CHEMISTRY OF MATERIALS · MARCH 2009

Impact Factor: 8.35 · DOI: 10.1021/cm803037g

CHEMISTRY OF MATERIALS

Article

Covalent Functionalization of Short, Single-Wall Carbon Nanotubes: Photophysics of 2,4,6-Triphenylpyrylium Attached to the Nanotube Walls

Carmela Aprile, Roberto Marti#n, Mercedes Alvaro, Hermenegildo Garcia, and J. C. Scaiano

Chem. Mater., **2009**, 21 (5), 884-890• DOI: 10.1021/cm803037g • Publication Date (Web): 29 January 2009

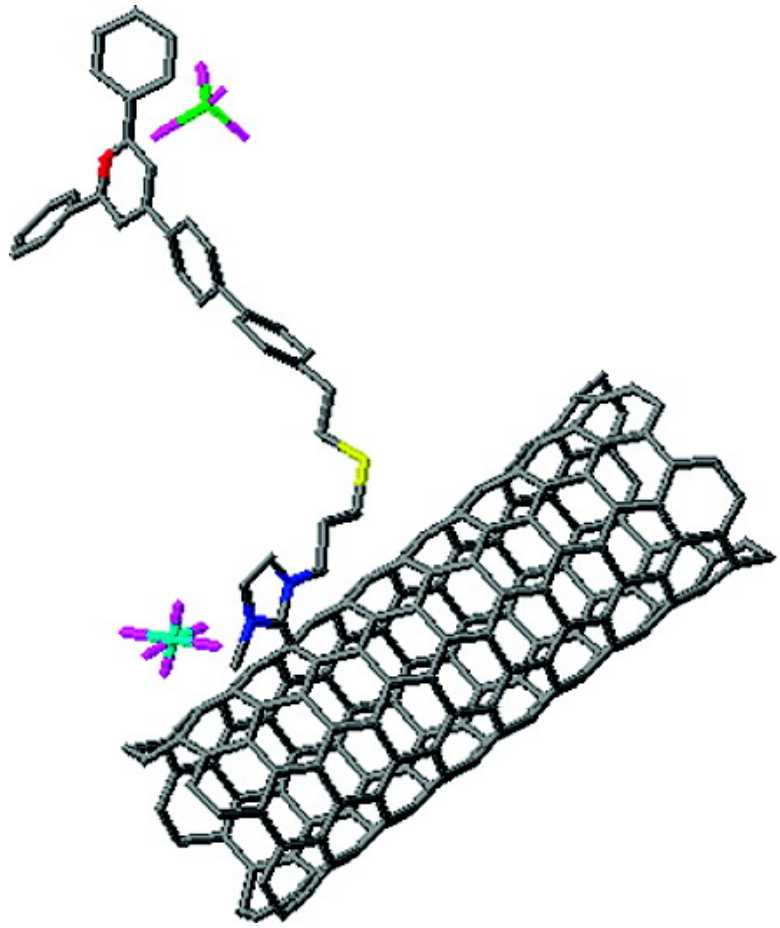

More About This Article

Additional resources and features associated with this article are available within the HTML version:

Chemistry of Materials is published by the American Chemical Society. 1155 Sixteenth Street N.W., Washington, DC 20036

Covalent Functionalization of Short, Single-Wall Carbon Nanotubes: Photophysics of 2,4,6-Triphenylpyrylium Attached to the Nanotube Walls

Carmela Aprile,[†] Roberto Martín,[†] Mercedes Alvaro,[†] Hermenegildo Garcia,*[,†] and J. C. Scaiano*[,‡]

Instituto de Tecnología Química CSIC-UPV, Universidad Politécnica de Valencia, Avenida De los Naranjos s/n, 46022 Valencia, Spain, and Center for Catalysis Research and Innovation, Department of Chemistry, University of Ottawa, 10 Marie Curie, Ottawa K1N 6N5, Canada

Received November 7, 2008. Revised Manuscript Received December 23, 2008

2,4,6-Triarylpyrylium units (TP^+) have been attached covalently to the walls of short, water-soluble single-wall carbon nanotubes (sSWNT) to give TP-sSWNT sample (6.8 wt % on TP^+). The high loading achieved in this manner has allowed characterization of the material by a wide range of techniques, including AFM (about 1 μm length), thermogravimetric analyses (absence of inorganic particles in the sample), Raman spectroscopy (radial breathing vibration mode at 180 cm^{-1}), and solution ^1H NMR spectroscopy (up to 0.5 ppm variation in the δ of the protons upon attachment to the graphene walls). Optical spectroscopy reveals the absence of the van Hove singularities in the TP-sSWNT sample. Fluorescence spectroscopy indicates sSWNT quenching of the otherwise intense TP^+ emission. Laser flash photolysis has allowed detecting a transient species characterized by a broad absorption from 400 to 700 nm that decays with a fast (<500 ns) and a slow (a few microsecond) kinetics. TP-sSWNT emits NIR luminescence with an estimated 2.3×10^{-3} quantum yield.

Introduction

Covalent functionalization of short, soluble, single-wall carbon nanotubes (sSWNT) is a topic of much current interest.[1−7] The semiconducting properties inherent to SWNT are well-suited to interact either with electron donor or acceptor molecules.[8−10] The narrow band gap of sSWNT makes possible either injection of electrons into its conduction or abstraction of electrons from its valence band, respectively.[11] Although there are numerous reports about the functionalization with electron donor substituents,[12−17] functionalization with electron acceptor moieties has been considerably less studied.[18,19] Recently we have reported sSWNT functionalization by 2,4,6-triphenylpyryliums (TP^+) attached through amide linkages to the carboxylic groups of the SWNT present at the tips and wall defects of the nanotube.[19] This methodology has as a drawback the limited loading of TP^+ photosensitizer (3 wt %) that can be introduced because of the low density of carboxylic groups present in the SWNT. To obtain highly responsive sSWNT derivatives, it would be desirable to achieve a higher percentage of functionalization. This can be accomplished by designing alternative synthetic approaches based on the reactivity of the graphene walls rather than on the carboxylic groups.[7]

In this article, we describe the synthesis and photophysical properties of a sSWNT functionalized with higher loading of photoresponsive TP^+ attached to the graphene walls. Extensive functionalization on the walls could change the electronic properties of the resulting molecules, decreasing the electronic conductivity of the carbon nanotube and increasing its band gap.[16] For this reason wall functionalization and variation of TP^+ loading and semiconducting

* Corresponding author. E-mail: tito@photo.chem.uottawa.ca (J.C.S.); hgarcia@qim.upv.es (H.G.).
[†] Universidad Politécnica de Valencia.
[‡] University of Ottawa.

(1) Bahr, J. L.; Tour, J. M. *J. Mater. Chem.* **2002**, *12*, 1952.
(2) Dyke, C. A.; Tour, J. M. *Nano Lett.* **2003**, *3*, 1215.
(3) Dyke, C. A.; Tour, J. M. *J. Am. Chem. Soc.* **2003**, *125*, 1156.
(4) Hirsch, A. *Angew. Chem., Int. Ed.* **2002**, *41*, 1853.
(5) Sun, Y. P.; Fu, K. F.; Lin, Y.; Huang, W. J. *Acc. Chem. Res.* **2002**, *35*, 1096.
(6) Niyogi, S.; Hamon, M. A.; Hu, H.; Zhao, B.; Bhowmik, P.; Sen, R.; Itkis, M. E.; Haddon, R. C. *Acc. Chem. Res.* **2002**, *35*, 1105.
(7) Tasis, D.; Tagmatarchis, N.; Bianco, A.; Prato, M. *Chem. Rev.* **2006**, *106*, 1105.
(8) Avouris, P. *Acc. Chem. Res.* **2002**, *35*, 1026.
(9) Dai, H. J. *Acc. Chem. Res.* **2002**, *35*, 1035.
(10) Ouyang, M.; Huang, J. L.; Lieber, C. M. *Acc. Chem. Res.* **2002**, *35*, 1018.
(11) Guldi, D. M.; Rahman, G. M. A.; Zerbetto, F.; Prato, M. *Acc. Chem. Res.* **2005**, *38*, 871.
(12) Ballesteros, B.; de la Torre, G.; Ehli, C.; Rahman, G. M. A.; Agullo-Rueda, F.; Guldi, D. M.; Torres, T. *J. Am. Chem. Soc.* **2007**, *129*, 5061.
(13) Campidelli, S.; Sooambar, C.; Diz, E. L.; Ehli, C.; Guldi, D. M.; Prato, M. *J. Am. Chem. Soc.* **2006**, *128*, 12544.
(14) Ehli, C.; Rahman, G. M. A.; Jux, N.; Balbinot, D.; Guldi, D. M.; Paolucci, F.; Marcaccio, M.; Paolucci, D.; Melle-Franco, M.; Zerbetto, F.; Campidelli, S.; Prato, M. *J. Am. Chem. Soc.* **2006**, *128*, 11222.
(15) Herranz, M. A.; Martin, N.; Campidelli, S.; Prato, M.; Brehm, G.; Guldi, D. M. *Angew. Chem., Int. Ed.* **2006**, *45*, 4478.
(16) Herranz, M. A.; Ehli, C.; Campidelli, S.; Gutierrez, M.; Hug, G. L.; Ohkubo, K.; Fukuzumi, S.; Prato, M.; Martin, N.; Guldi, D. M. *J. Am. Chem. Soc.* **2008**, *130*, 66.
(17) Alvaro, M.; Atienzar, P.; la Cruz, P.; Delgado, J. L.; Troiani, V.; Garcia, H.; Langa, F.; Palkar, A.; Echegoyen, L. *J. Am. Chem. Soc.* **2006**, *128*, 6626.
(18) Alvaro, M.; Aprile, C.; Atienzar, P.; Garcia, H. *J. Phys. Chem. B* **2005**, *109*, 7692.

10.1021/cm803037g CCC: $40.75
Published on Web 01/29/2009

Scheme 1. Synthetic Route Followed To Prepare Pyrylium 4 Having a Terminal *N*-Methylimidazolium Tag

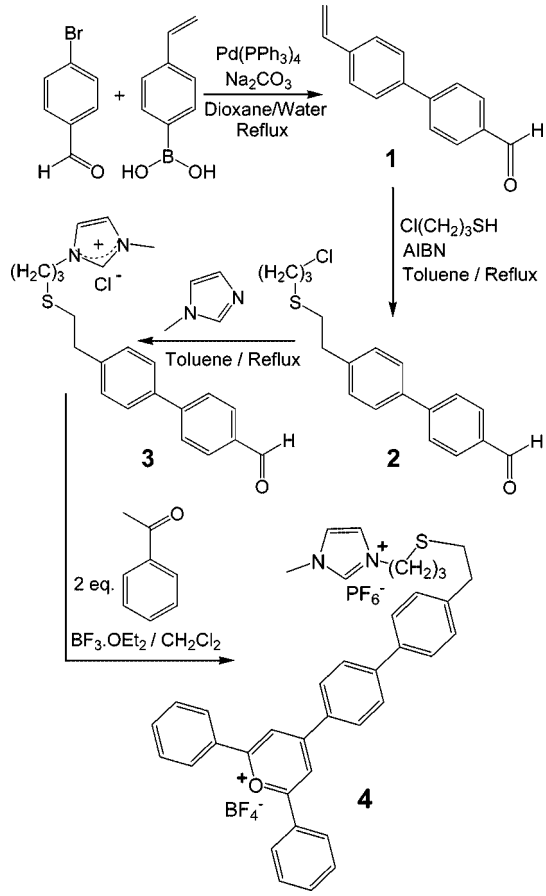

properties of sSWNT could render a derivative that exhibits distinctive properties from those of the congener obtained through carboxylic group derivatization that has lower loading and a larger fraction of intact graphene walls.

Results and Discussion

Our synthetic approach is based on the nitrogen heterocyclic carbene insertion into SWNT graphene walls.[7] This synthetic route requires the preparation of the *N*-methylimidazolium derivative of TP^+ **4** that was obtained by formation of the pyrylium heterocycle from acetophenone and biphenyl carbaldehyde **3**. The synthetic intermediate **3** was obtained from N-methylimidazolium and 4-(ω-chloropropylthio)ethylbiphenyl **2**. Scheme 1 presents the actual reaction steps followed for the synthesis of TP^+ connected to an imidazolium tag **4**.

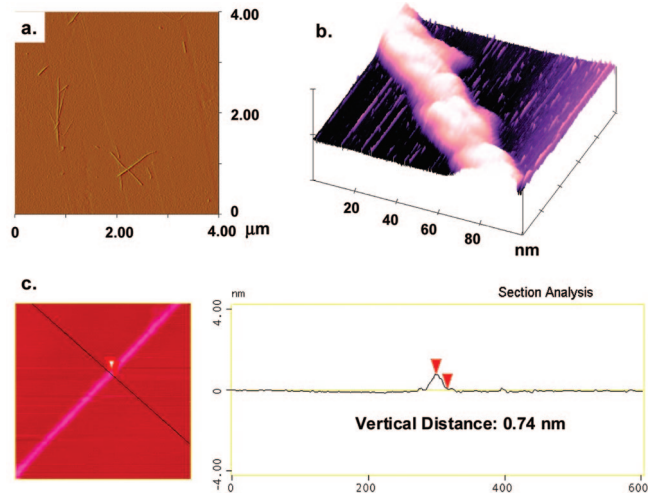

Figure 1. (a, b) AFM images of TP-sSWNT at two different magnifications and (d) cross-section of the tube according to image c showing the height of the nanotube.

Prior to the covalent attachment of the TP^+ imidazolium derivative **4** to sSWNT, we submitted the commercially available high-pressure carbon monoxide (HiPCO) SWNT to the oxidative treatment with concentrated HNO_3/H_2SO_4 acid mixture followed by sonication for 60 min.[20,21] Working under controlled conditions it was possible to obtain a purified sSWNT sample with an average length of about 1 μm.[21] The pyrylium derivative **4** was attached to the sSWNT by reacting it with K^{t}BuO. Scheme 2 shows the procedure used to prepare the sSWNT sample having triarylpyrylium units attached to the walls (TP-sSWNT). Figure 1 shows selected atomic force microscopy images of the resulting TP-sSWNT sample prepared in this work.

As already reported, one of the main consequences of chemical treatment under the harsh acid conditions used to purify and cut the commercial sample is the high water solubility (2 mg mL^{-1}) of the resulting purified sSWNT, that forms indefinitely persistent colloidal suspensions in water.[20] This high water solubility derives from the relatively short length and the presence of carboxylic groups and other oxygen functionalities at the tips and on the wall defects of the material. After the synthesis, the resulting TP-sSWNT sample was significantly less water-soluble than the original sSWNT, indicating that substituents on the walls have an adverse effect on the aqueous solubility.

The defects on the graphene walls of sSWNT are manifested in the Raman spectra of the samples (Figure 2). Compared to the original HiPCO SWNT or parent sSWNT,

Scheme 2. Reaction of Pyrylium 4 with sSWNT to form TP-sSWNT

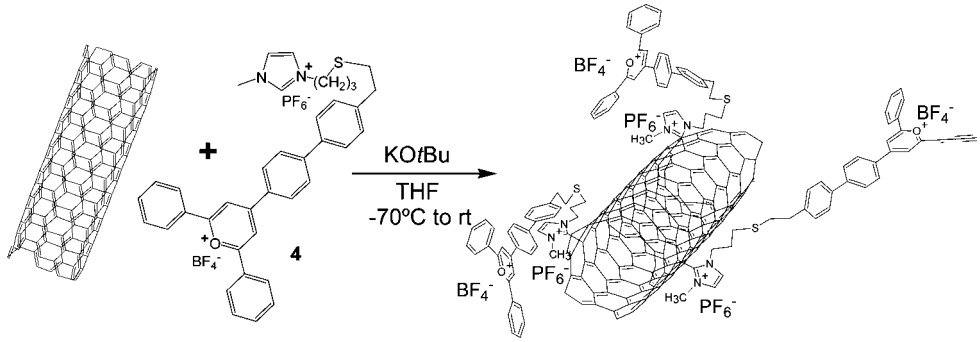

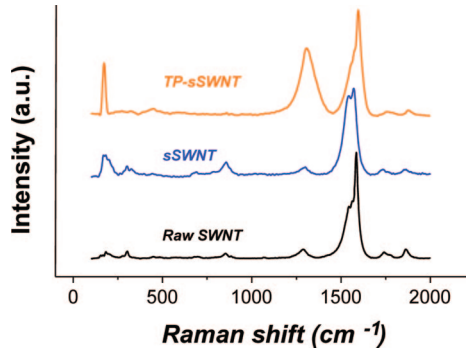

Figure 2. Raman spectra of raw SWNT, sSWNT, and TP-sSWNT recorded at 100 °C.

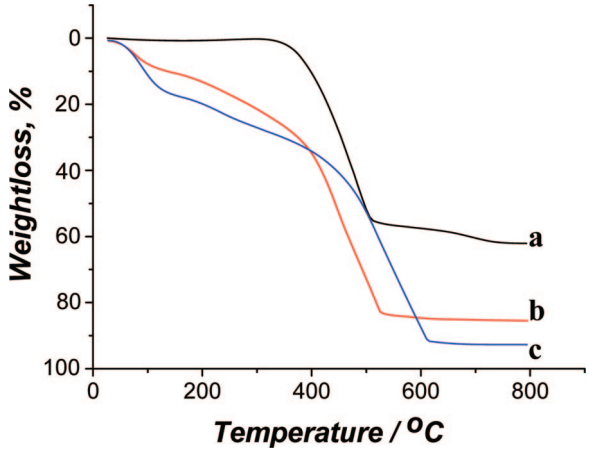

Figure 3. TGA of (a) raw SWNT, (b) sSWNT, and (c) TP-sSWNT.

covalent functionalization on the graphene walls leads for TP-sSWNT to a decrease on the relative intensity of the tangential vibration mode at around 1600 cm^{-1} with a concomitant increase of the band at 1300 cm^{-1}. This feature is typical of wall functionalization. The characteristic breathing radial vibration mode specific of single walled nanotubes appearing at around 180 cm^{-1} is still clearly present in TP-sSWNT.

The success of purification with removal of the catalyst particles used to obtain HiPCO SWNT is confirmed by thermogravimetric analysis (TGA). Figure 3 shows the thermogravimetric profiles of raw SWNT, purified sSWNT, and functionalized TP-sSWNT. As it can be seen in this figure, the original HiPCO SWNT sample upon combustion still retains about the 50% of the initial weight, indicating the presence of inorganic particles that cannot be burned at high temperatures in the presence of air. In contrast, TGA shows that sSWNT undergoes almost complete combustion and about 90% of sample weight is lost at temperatures below 700 °C. Analogously, TP-sSWNT losses almost 100% of the sample weight upon thermal treatment under air.

The loading of TP^+ in TP-sSWNT can be obtained from the comparison of the TGA profiles of sSWNT and TP-sSWNT, by considering that water desorption and combustion of the pyrylium substituent takes place at lower temperature than the combustion of the sSWNT. Thus, the difference in weight loss for sSWNT and TP-sSWNT occurring at temperatures of about 300 °C is attributed to the presence of TP^+. Alternatively, we determined the loading of TP^+ by elemental combustion chemical analysis of TP-sSWNT considering that N and S elements, absent in sSWNT, are introduced in the linker during nanotube functionalization. In this way, it was estimated that the TP^+ content in TP-sSWNT is 6.8 wt %. This value is significantly higher than the 3 wt % previously reported for an analogous material containing TP^+ through peptide bonds[19] and shows the advantage of devising functionalization strategies based on the reactivity of the graphene wall in order to achieve a high degree of substitution.

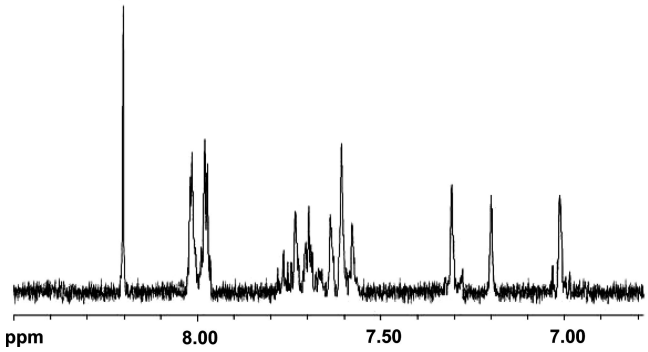

Figure 4. Expansion of the aromatic region of the 300 MHz ^1H NMR spectrum of TP-sSWNT in d_6-DMSO.

Important evidence in support of the covalent functionalization in TP-sSWNT was solution ^1H NMR spectroscopy. The relatively high solubility of TP-sSWNT allows recording of the ^1H NMR spectrum in d_6-DMSO. Figure 4 shows the aromatic region of TP-sSWNT in which the low-field singlet characteristic of the equivalent hydrogens at the 3 and 5 positions of the positively charged pyrylium ring appears at 8.4 ppm. Typically, the δ value of these Hs for many triarylpyrylium compounds is recorded at about 9 ppm and in the case of precursor **4**, they appear at 9.1 ppm. We propose that the notable upfield shift (from 9.1 in compound **4** to 8.4 ppm in TP-sSWNT) is due to the magnetic anisotropy created by the proximity of the nanotube graphene walls to these hydrogens upon covalent attachment to the walls. Therefore, this variation in the δ value of the hydrogens of the pyrylium ring can be taken as a ^1H NMR spectroscopic evidence of the spatial proximity between the triarylpyrylium and the walls in TP-sSWNT arising from the covalent attachment. The other signals recorded in the aromatic region, and particularly the doublet of the phenylene ring *o*-hydrogens at 8.00 ppm and the singlet at 7.0 ppm of the imidazolium ring, are compatible with the structure of TP-sSWNT. The variations in the chemical shifts from the precursor pyrylium **4** are remarkable and again are attributed to the influence of the graphene wall of sSWNT on the lateral substituent. Spectra with such high resolution as that of Figure 4 are rare; this paucity of ^1H NMR data frequently reflects solubility problems. In our case, the high solubility

(19) Alvaro, M.; Aprile, C.; Ferrer, B.; Garcia, H. *J. Am. Chem. Soc.* **2007**, *129*, 5647.
(20) Hudson, J. L.; Casavant, M. J.; Tour, J. M. *J. Am. Chem. Soc.* **2004**, *126*, 11158.
(21) Liu, J.; Rinzler, A. G.; Dai, H. J.; Hafner, J. H.; Bradley, R. K.; Boul, P. J.; Lu, A.; Iverson, T.; Shelimov, K.; Huffman, C. B.; Rodriguez-Macias, F.; Shon, Y. S.; Lee, T. R.; Colbert, D. T.; Smalley, R. E. *Science* **1998**, *280*, 1253.

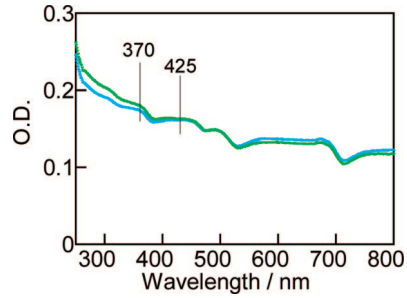

Figure 5. Transmission optical spectra of TP-sSWNT in D_2O (1.32 μg mL^{-1}) before (blue, lower trace at 300 nm) and after (green, upper plot at 300 nm) laser flash photolysis. The absorption bands characteristic of TP^+ chromophore present in TP-sSWNT have been indicated.

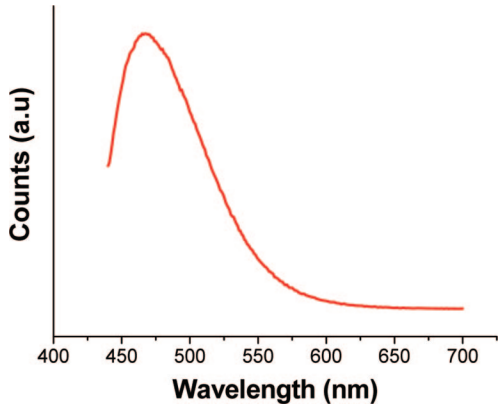

Figure 6. Fluorescence spectrum of an acetonitrile solution of TP-sSWNT (1.0 μg mL^{-1}, λ_{ex} 420 nm).

of TP-sSWNT in DMSO is responsible for the quality of this spectrum recorded in solution.

The information from optical spectroscopy is relevant in order to understand the photophysical properties of TP-sSWNT. As expected in view of the absorption spectra of sSWNT and TP^+, the spectrum of TP-sSWNT exhibits a continuum absorption that increases toward short wavelengths on the top of which appear the characteristic absorption band of TP^+ chromophore with maxima at 370 and 420 nm (Figure 5). The van Hove singularities characteristic of sSWNT are lacking in our TP-sSWNT sample. There are some precedents where upon cutting and functionalization of SWNT the van Hove singularities disappear.[22−24] Thus, in our case, the absence of absorption bands above 800 nm is a reflection of the short length and wall functionalization of our sample.

Photophysics of TP-sSWNT. Upon excitation at 420 nm TP^+ normally emits an intense fluorescence (Φ 0.33) at 550 nm.[25] In our case we have been able to observe a weak fluorescence from TP-sSWNT (Figure 6). The interaction between TP^+ and the walls of SWNT should be responsible for the quenching of this emission. This quenching is reflected in the fact that the emission quantum yield of TP-sSWNT is extremely low (Φ 0.01). There are numerous precedents in the literature reporting SWNT quenching of the emission from several fluorescent molecules.[26−30]

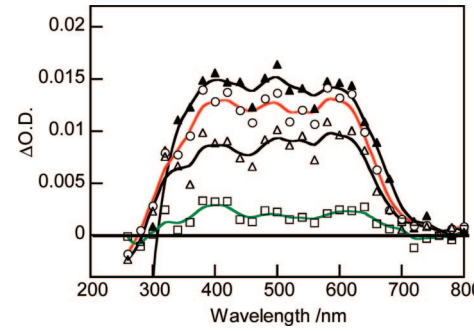

Figure 7. Time-resolved transmission optical spectra for a N_2-purged D_2O solution of TP-sSWNT (1.32 μg mL^{-1}) upon 355 nm laser excitation (3 mJ $pulse^{-1}$) recorded at 120 (▲), 170 (○), 250 (Δ), and 850 (□) ns after the laser flash. The continuous lines correspond to a smooth fitting of the experimental points.

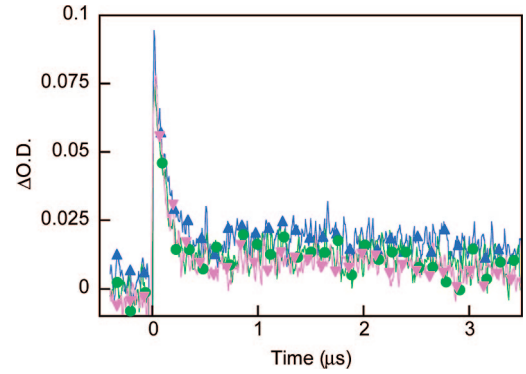

Figure 8. Temporal profile of the signal monitored at 450 (▲), 550 (•), and 650 (▼) nm upon 355 nm laser excitation (3 mJ $pulse^{-1}$) of a N_2-purged D_2O solution of TP-sSWNT (1.32 μg mL^{-1}).

Laser flash photolysis is a powerful technique for the detection and characterization of electronic excited states and to provide evidence of the interaction of these excited states with quenchers. In the particular case of TP-sSWNT, it is of interest to establish whether or not light absorption leads to a transient species arising from the interaction between the two moieties (TP and sSWNT) of this structure. To address this point, we used 355 nm laser excitation of TP-sSWNT in solution. Figure 7 shows the transient absorption spectra obtained, whereas the temporal profile of the signal at the different wavelengths is shown in Figure 8. As can be seen in Figure 7, the spectra are characterized by a very broad featureless absorption from 400 to 700 nm accompanied by a negative signal in the 280−350 nm region at shorter delay times. This negative signal is probably due to the bleaching of the ground state. It should be noted that the optical

(22) Saito, R.; Kataura, H. *Carbon Nanotubes* **2001**, *80*, 213.
(23) Ryabenko, A. G.; Kiselev, N. A.; Hutchison, J. L.; Moroz, T. N.; Bukalov, S. S.; Mikhalitsyn, L. A.; Loutfy, R. O.; Moravsky, A. P. *Carbon* **2007**, *45*, 1492.
(24) Lee, K. J.; Lee, H.; Lee, J. Y.; Lim, S. C.; An, K. H.; Lee, Y. H.; Lee, Y. S. *J. Kor. Phys. Soc.* **2005**, *46*, 906.
(25) Montes-Navajas, P.; Teruel, L.; Corma, A.; Garcia, H. *Chem. Eur. J.* **2008**, *14*, 1762.
(26) Chu, S. S.; Yi, W. H.; Wang, S. F.; Li, F. M.; Feng, W. K.; Gong, Q. H. *Chem. Phys. Lett.* **2008**, *451*, 116.
(27) Chitta, R.; Sandanayaka, A. S. D.; Schumacher, A. L.; D'Souza, L.; Araki, Y.; Ito, O.; D'Souza, F. *J. Phys. Chem. C* **2007**, *111*, 6947.
(28) Qu, L. W.; Martin, R. B.; Huang, W. J.; Fu, K. F.; Zweifel, D.; Lin, Y.; Sun, Y. P.; Bunker, C. E.; Harruff, B. A.; Gord, J. R.; Allard, L. F. *J. Chem. Phys.* **2002**, *117*, 8089.
(29) Alvaro, M.; Atienzar, P.; Bourdelande, J. L.; Garcia, H. *Chem. Phys. Lett.* **2004**, *384*, 119.
(30) Gomez-Escalonilla, M. J.; Atienzar, P.; Garcia Fierro, J. L.; Garcia, H.; Langa, F. *J. Mater. Chem.* **2008**, *18*, 1592.

absorption of TP-sSWNT solutions is stronger at shorter wavelengths.

Coincidence of the temporal profile of the signal at different wavelengths from 450 to 700 nm indicates that the transient spectrum probably corresponds to a single species, particularly considering that the signal profile is complex. The signal decay exhibits two components. One of them decays fast in a few hundreds of nanoseconds. The second component exhibits a growth in the first microsecond after the laser pulse and is considerably much longer lived. The short-lived signal can be adequately fit to a first-order kinetics with a half-life of 0.5 μs.

Given the well-established ability of excited TP^+ to act as electron acceptor[31] and the ability of sSWNT to act as electron donor,[15,18,28,30] the most reasonable assignment of the transient spectra of Figure 7 is the charge-separated state arising from photoinduced electron transfer. Considering that 355 nm can excite both TP^+ and sSWNT, charge separation could be promoted by light excitation of either of the two chromophores. We note that TP$^{\cdot}$ radical that should be generated in the photoinduced electron transfer is characterized by a weak absorption peak at 540 nm.[31] However, this weak absorption is difficult to observe and has frequently gone undetected when photoinduced electron transfer leading to TP$^{\cdot}$ gives a concomitant rise of another species exhibiting a much stronger absorption. In other words, the spectrum shown in Figure 7 contains information mainly about the positive hole and can be assumed that it is localized in the sSWNT moiety. The two components in the transient decay would then correspond to two different regimes of the charge recombination. It has been observed that collapse of the charge separated states by electron and hole recombination can occur in different length scales from picosecond for geminate radical ion pairs to microsecond or longer for separate ion pairs depending of the proximity and distance of the charge separation.[32]

It has been recently proposed that bleaching and recovery of the van Hove functionalities can be used as a fingerprint for the occurrence of photoinduced electron transfer involving SWNT.[12,33] However, in our case, the fact that the TP-sSWNT does not exhibit van Hove singularities in the ground-state optical spectrum prevents their use.

NIR Emission of TP-sSWNT. It has been observed that diluted D_2O solutions of sSWNT exhibits a relatively strong emission in the NIR region.[34] It can be anticipated that functionalization can be a strategy to modulate the NIR emission inherent to SWNT. For this reason, we wanted to determine the NIR emission of TP-sSWNT, trying to correlate its efficiency to that for the parent sSWNT to establish the influence of the TP^+ units. sSWNT emits in the NIR with a quantum yield of 3.9×10^{-3} and with 30 μs lifetime. Development of novel materials exhibiting strong NIR emission is of much current applied interest.[35,36]

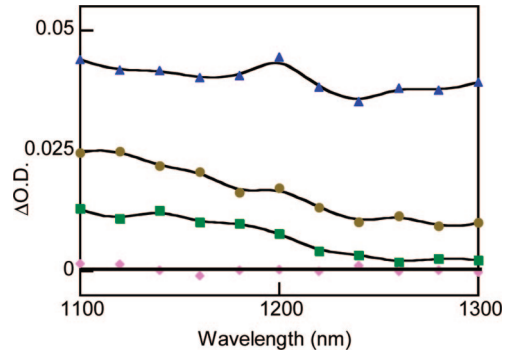

Figure 9. NIR emission spectra recorded 5, 12, 23, and 100 μs (from top to bottom) after 266 nm laser excitation of D_2O TP-sSWNT solution (2.6 μg mL^{-1}).

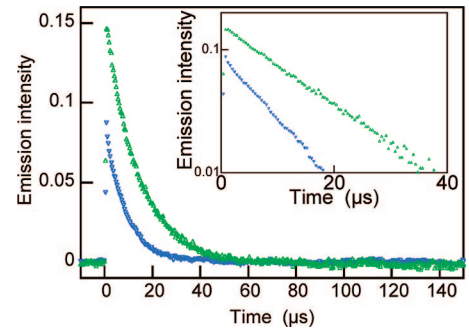

Figure 10. Signal decay monitored at 1300 nm after 266 nm excitation of optically matched sSWNT (upper trace in green, 1.11 μg mL^{-1}) and TP-sSWNT (lower trace in blue, 2.6 μg mL^{-1}) solutions in D_2O. Inset: semilogarithm plot of the decays.

In the case of TP-sSWNT, we have been able to observe NIR emission in the 1100−1500 nm region upon excitation at 266 nm (Figure 9). This emission is analogous to that of unfunctionalized sSWNT.[34] Interestingly, Φ of optically matched solutions was 1.72 weaker for TP-sSWNT relative to sSWNT. We suggest that the difference in the NIR emission quantum yield between unfunctionalized sSWNT and TP-sSWNT derives from the electron transfer between sSWNT and TP^+ that causes the quenching of the excited-state localized on sSWNT and eventually leads to radiationless decay.

The temporal profiles of the NIR emision of sSWNT and TP-sSWNT were similar (Figure 10). The decay of the TP-sSWNT NIR emission fits well to a first-order kinetics with a 20.2 μs lifetime.

2,4,6-Triphenylpyrylium tetrafluoroborate ($TPBF_4$) not covalently bound to sSWNT also quenches in submicromolar concentrations the NIR emission of sSWNT.[34] Comparing $TPBF_4$ quenching on the NIR sSWNT emission with the emission of TP-sSWNT for comparable TP^+ and sSWNT concentrations under otherwise identical conditions, it can be concluded that covalently bound TP^+ is less effective as quencher than unbound $TPBF_4$. It is possible that the lower quenching efficiency of covalently bound TP^+ is due to the

(31) Miranda, M. A.; García, H. *Chem. Rev.* **1994**, *94*, 1063.
(32) Kavarnos, G. J.; Turro, N. J. *Chem. Rev.* **1986**, *86*, 401.
(33) Angeles Herranz, M.; Ehli, C.; Campidelli, S.; Gutierrez, M.; Hug, G. L.; Ohkubo, K.; Fukuzumi, S.; Prato, M.; Martin, N.; Guldi, D. M. *J. Am. Chem. Soc.* **2008**, *130*, 66.
(34) Aprile, C.; Martín, R.; Alvaro, M.; Scaiano, J. C.; Garcia, H. manuscript in preparation.
(35) Kazaoui, S.; Minami, N.; Nalini, B.; Kim, Y.; Hara, K. *J. Appl. Phys.* **2005**, 98.
(36) Carlson, L. J.; Krauss, T., D *Acc. Chem. Res.* **2008**, *41*, 235.

restricted mobility of this quencher when covalently bound as compared to the free molecule. We notice, however, that the damage to the graphene wall due to the functionalization can also contribute to the weaker quenching effect observed for TP-sSWNT compared to the more efficient intermolecular $TPBF_4$ quenching of sSWNT.

Experimental Section

^{1}H NMR and ^{13}C NMR spectra were recorded on a Bruker 300 apparatus using CD_3CN or [D_6]-DMSO as solvents. Chemical shifts are given in parts per millions and TMS was used as internal standard for ^{1}H NMR spectroscopy. UV−vis absorption spectra were obtained in acetonitrile using quartz cuvettes on a Shimadzu spectrophotometer. FT-IR spectra were recorded on a Nicolet Impact 410 spectrophotometer using KBr disks or self-supported wafers compressed to 2 Ton cm^{-2} for 2 min. Raman spectra were recorded at room temperature at the ambient atmosphere using a Renishaw in Via Microscope with diode laser (785 nm) and averaging 10 scans of different areas of the black solid.

Atomic force microscopy images were obtained with a multimode system equipped with a Nanoscope III A controller. Thermogravimetric analyses from room temperature to 900 °C were performed in a Netsch Thermobalance under air flow using kaolin as inert reference.

Fluorescence spectra were recorded in a PTI spectrofluorimeter using septum-capped Suprasil quartz cuvettes after purging the samples with nitrogen for at least 15 min before the experiments. Laser flash photolysis experiments were carried out using a LuzChem LFP-111 System and the third harmonic of a Nd/YAG laser (Minilite-II 355 nm, 7 ns fwhp, 8 mJ pulse^{-1}) as excitation source. The samples were diluted up to an absorbance around 0.2 units and then contained in 1 × 1 cm^2 cuvettes capped with septa, they were purged with N_2 or O_2 for at least 15 min before the measurements.

NIR emission studies were carried out using a Peltier-cooled (−62 °C) Hamamatsu NIR detector operating at 900 V coupled with a computer-controlled grating monochromator. For excitation, the third harmonic (355 nm, 7 ns fwhh, 50 mJ × pulse^{-1}) of the primary beam of a Nd:YAG laser or an Nd:YAG pumped OPO operating at 540 nm (7 ns fwhh, 40 mJ pulse^{-1}) were used. The solutions were placed in a 1 × 1 cm^2 Suprasil quartz cuvettes capped with septa. The solutions were purged with N_2 or O_2 for at least 15 min before the laser experiments. The system was controlled with a PC computer using LuzChem LFPv3 software.

Materials. The single walled carbon nanotubes samples used in this study having 80−90% relative carbonaceous purity was of HiPCO (High pressure carbon monoxide) type and were obtained from Carbolex (www.carbolex.com)

Purification of SWNTs. Purification of SWNT to remove the inorganic catalyst particles was carried out by treatment with hot nitric acid under controlled conditions. In detail, 1 g of raw SWNT was refluxed in 500 mL 3 M HNO_3 at 120 °C for 12 h. The nitric acid concentration, time and reaction temperature employed were selected for this sample to optimize purification without massive damage of the nanotubes. Samples of different origin require to adapt these conditions to optimize the oxidative nanotubes cut. After treatment with hot nitric acid, the mixture was cooled to room temperature and diluted with distilled water. Several consecutive cycles of centrifugation-redispersion in Milli-Q water were performed to remove the excess of acid. After five cycles the filtrate pH value was neutral. Finally, the treated purified SWNT was submitted to freeze-drying solvent removal under vacuum to obtain a dust-like black material. The efficiency of the inorganic particle removal process was checked by TG analysis that showed almost complete combustion of the carbonaceous sample.

Cutting of SWNTs. Soluble, short SWNT were obtained from purified SWNT by an oxidative process in strong acid medium that produces initial sidewall damage followed by rapid oxidative cutting around the created wall defect forming carboxylic groups. To effect the cutting, acid suspensions of purified HiPCO SWNT were submitted to ultrasonication/heating treatment. The required acid solutions (3:1, vol/vol 96% H_2SO_4/30% HNO_3) were prepared immediately prior to use. In this way, 150 mg of purified SWNTs were sonicated at 60 °C in 8 mL of the acid mixture during 45 min. After this time, the acid excess was removed by five consecutive cycles of centrifugation-redispersion in Milli-Q water. SWNT was finally obtained by freeze-drying under vacuum. The average length of soluble sSWNT estimated by TEM microscopy is 500 nm.

Preparation of 4′-Vinyl-1,1′-biphenyl-4-carbaldehyde (1). 4-Bromobenzaldehyde (1 g, 5.4 mmol), 4-vinylphenylboronic acid (1.6 g, 10.8 mmol), ground potassium carbonate (g, 108 mmol) and [$Pd(PPh_3)_4$](624 mg, 0.54 mmol, 10 mol Pd%) in dioxane (40 mL) were stirred magnetically in a preheated oil bath at 110 °C for 48 h under nitrogen atmosphere. After this time, the suspension was filtered while hot under vacuum and the solvent was evaporated under vacuum. The crude residue was submitted to partition in CH_2Cl_2/water, the organic phase was collected, dried, and CH_2Cl_2 evaporated under reduced pressure. The brownish crude product was purified by column chromatography (CH_2Cl_2) to obtain a bright-green solid (0.75 g, 66.7%)

^{1}H NMR (300 MHz, $CDCl_3$): δ (ppm) = 10.03 (s, 1H), 7.93 (d, 2H, J = 7.8 Hz), 7.74 (d, 2H, J = 8.4 Hz), 7.60 (d, 2H, J = 8.4 Hz), 7.50 (d, 2H, J = 8.4 Hz), 6.75 (dd, 1H, J_1 = 17.4 Hz, J_2 = 10.51 Hz), 5.86 (d, 1H,, J = 17.4 Hz), 5.31 (d, 1H,, J = 10.8 Hz); ^{13}C NMR (300 MHz, $CDCl_3$): δ (ppm) = 191.87, 146.63, 138.91, 137.78, 136.09, 135.15, 130.28, 127.47, 127.42, 126.83, 114.75; IR (KBr): ν (cm^{-1}) = 3047, 2965, 2974, 2807, 2719, 1920, 1770, 1695, 1592, 1497, 1388, 1299, 1204, 1162, 1107, 992, 917, 821. 691.

Synthesis of 4′-{2-[(3-Chloropropyl)thio]ethyl}−1,1′-biphenyl-4-carbaldehyde (2). 3-Chloropropanthiol (2.8 mL, 29.6 mmol) was added to a solution of compound **1** (1.54 g, 7.4 mmol) and AIBN (150 mg, 10%) in degassed dry toluene (10 mL). After stirring at 110 °C for 24 h, the solvent was removed in vacuo and the crude product was purified by column chromatography (CH_2Cl_2/Hexane, 7:3) to obtain **2** (1.65 g, 69.9%) was obtained as a green oil.

^{1}H NMR (300 MHz, $CDCl_3$): δ (ppm) = 10.06 (s, 1H), 7.97 (d, 2H, J = 8.4 Hz), 7.76 (d, 2H, J = 8.4 Hz), 7.61 (d, 2H, J = 8.4 Hz), 7.35 (d, 2H, J = 8.4 Hz), 3.67 (t, 2H, J = 7.2 Hz), 2.98 (t, 2H, J = 8.4 Hz), 2.86 (t, 2H, J = 6.9 Hz), 2.73 (t, 2H, J = 7.9 Hz), 2.09 (q, 2H, J = 6.9 Hz); ^{13}C NMR (300 MHz, $CDCl_3$): δ (ppm) = 191.89, 146.85, 140.87, 137.81, 135.07, 130.27, 129.20, 127.47, 127.44, 43.48, 35.82, 33.55, 32.17, 29.18; IR (KBr): ν (cm^{-1}) = 3040, 2924, 2835, 2739, 2357, 1913, 1695, 1606, 1497, 1442, 1395, 1305, 1297, 1210, 1169, 1005, 944, 807, 759, 698, 561, 507.

Obtainment of *N*-Methyl-*N*′-[4′-{2-[(3-chloropropyl)thio]ethyl}−1,1′-biphenyl-4-carbaldehyde] Imidazolyl Chloride (3). A solution of compound **2** (1.05 g, 3.29 mmol) and *N*-methylimidazole (265 μL, 3.29 mmol) in dry toluene (5 mL) was heated at reflux temperature under Ar for 48 h. The solvent was removed and diethyl ether was added. The suspension was stirred overnight to wash out *N*-methylimidazole and **2**. Compound **3** was obtained as brown oil (0.9 g, 68.1%).

^{1}H NMR (300 MHz, [D_6]-DMSO): δ (ppm) = 10.06 (s, 1H), 8.47 (s, 1H), 8.00 (d, 2H, J = 8.1 Hz), 7.87 (d, 2H, J = 8.1 Hz),

7.70 (d, 2H, $J = 8.1$ Hz), 7.44 (d, 2H, $J = 7.9$ Hz), 6.51 (s, 2H), 4.25 (t, 2H, $J = 7.2$ Hz), 3.87 (s, 3H), 2.95 (t, 2H, $J = 7.5$ Hz), 2.71 (t, 2H, $J = 7.2$ Hz), 2.59 (t, 2H, $J = 6.9$ Hz), 2.16 (q, 2H, $J = 6.9$ Hz); ^{13}C NMR (300 MHz, [D_6]-DMSO): δ (ppm) = 194,06, 146.50, 139.18, 133.04, 130.62, 129.79, 127.54, 126,62, 122.76, 50.54, 48.93, 38.11, 29.61, 27.10, 19.02; IR (KBr): ν (cm^{-1}) = 3101, 3040, 2931, 2850, 2732, 1688, 1600, 1402, 1217, 1169, 1114, 1012, 841, 739, 623, 555.

Mixed Hexafluorophosphate and Tetrafluoroborate Salt of 4-{[*N*-(*N′*-Methylmidazolylium)propylthio]ethylbiphenyl}2,6-diphenylpyrylium (4). 0.720 g (1.46 mmol) of compound **3** and 354 mg (2.92 mmol) of acetophenone were dissolved in 20 mL of acetonitrile in a 50 mL three necked flask under a dry nitrogen stream. To this solution, 0.5 mL (3.65 mmol) of boron trifluoride ethyl etherate was added at room temperature dropwise under magnetic stirring. After complete addition, the mixture was stirred at 90 °C for 24 h. Then, the solution obtained was cooled at room temperature and a mixture of ether and petroleum ether (2:1 v/v) was added to the solution to precipitate product **4**, which was thoroughly washed with ether and collected by filtration.

^{1}H NMR (300 MHz, $CDCl_3$): δ (ppm) = 10.2 (s, 2H), 9.29 (d, 2H, $J = 9.9$ Hz), 9.05 (s, 1H), 8.69 (d, 2H, $J = 9.9$ Hz), 8.13 (t, 2H, $J = 7.2$ Hz), 7.97 (d, 2H, $J = 7.2$ Hz), 7.84 (d, 2H, $J = 9.9$ Hz), 6.51 (s, 2H), 4.51 (t, 2H, $J = 6.9$), 3.19 (t, 2H, $J = 7.5$ Hz), 2.84 (t, 2H, $J = 6.9$), 2.39 (t, 2H, $J = 7.2$ Hz), 1.98 (t, 2H, $J = 7.2$ Hz); ^{13}C NMR (300 MHz, [D_6]-DMSO): δ (ppm) = 166.04, 163.81, 154.58, 153.34, 153.18, 146.91, 145.25, 140.45, 130.64, 127.8, 126.99, 123.38, 121.43, 111.78, 53.99, 39.51, 31.20, 28.31; IR (KBr): ν (cm^{-1}) = 3398, 3355, 3230, 3176, 2918, 2848, 2359, 2048, 1933, 1764, 1680, 1620, 1497, 1400, 1284, 1089, 1017, 814, 760, 697, 617, 511.

Synthesis of Sidewall-Functionalized TP-sSWNT. 0.200 g (0.25 mmol) of **4** was dissolved in 20 mL of anhydrous THF in a 50 mL three necked flask under Ar atmosphere. 375 μL (1.5 eq) of a 1.0 M solution of potassium tert-butoxide in tetrahydrofuran were added at − 60 °C while stirring.

After filtration through Celite under dry ice/acetone cooling, the freshly prepared carbene solution (200-fold excess) was added to a SWNT dispersion in THF at - 60 °C. After stirring at - 60 °C for 3 h, the reaction mixture was slowly warmed to room temperature, then diluted with ethanol. The precipitated functionalized TP-sSWNT nanotubes were submitted to three consecutive cycles of centrifugation-redispersion in acetone, finally washed with ethanol and dried under vacuum.

Conclusions

Using the carbene insertion reaction we have been able to prepare a sSWNT containing about 6.8 wt% of pyrylium chromophore attached to the graphene walls of sSWNT. This high loading allows the characterization of the resulting material by different techniques including solution ^{1}H NMR spectroscopy. The photochemical properties of TP-sSWNT material derives either from the electron acceptor ability of pyrylium (observation of photoinduced electron transfer) or from the s-SWNT subunits (NIR emission).

Acknowledgment. Financial support by the Spanish DGI (CTQ06-06859) and Canadian NSERC and CFI funding agencies is gratefully acknowledged. C.A. and R.M. also thank the Spanish Ministry of Science and Education for a Juan de la Cierva research associate contract and a postgraduate scholarship, respectively. H.G. (PR2007-0272) also acknowledges financial support for his stay at the University of Ottawa. Thanks are due to Michel Grenier for technical assistance.

CM803037G